



Charged gravastars with conformal motion in the Finslerian space-time

T. Sanjay^{1,a}, S. K. Narasimhamurthy^{1,b}, Z. Nekouee^{2,c}, H. M. Manjunatha^{1,d}

¹ Department of PG Studies and Research in Mathematics, Kuvempu University, Shankaraghata, Shivamogga, Karnataka 577 451, India

² School of Physics, Damghan University, Damghan 3671641167, Iran

Received: 13 September 2023 / Accepted: 30 March 2024

© The Author(s) 2024

Abstract In this article, we investigate the charged gravastar under conformal motion with the background of Finsler geometry. Mazur and Mottola pioneered the concept of the gravastar (gravitational vacuum star) for the first time. This vacuum object consists of three distinct regions, that is, (i) interior de Sitter region, (ii) thin shell consisting of ultrarelativistic stiff, and (iii) exterior vacuum Schwarzschild region. The nature of these regions can be analyzed by considering different equations of state parameters. We have studied various physical features of the gravastar, such as length, energy, entropy, stability, and the adiabatic index, both graphically and analytically within the Finslerian framework. Also, we have obtained the exact and non-singular solution for the gravastar model.

1 Introduction

The study of the black hole (BH), which is the result of the gravitational collapsing of compact stars (the endpoint of the stars), has the most significant importance in astrophysics and cosmology. Bardeen [1] obtained the exact solution for regular BH, and using a nonlinear electric field, Ayon-Beato et al. [2,3] extended the concept of regular BH. Due to the tremendous mass density and central singularity, it was arduous to study the structure of the black hole. To evade this event horizon and singularity, Mazur and Mottola [4,5] initiate a new solution for this gravitational collapse by elongating the idea of Bose-Einstein condensate to a gravitational system that is the alternative of BH known as a gravitational vacuum star (gravastar). These kinds of celestial objects are free

from any singularity and event horizon. The gravastar model proposed by Mazur and Mottola considered five zones. But Visser et al. [6] modified this model into three zones system, and these three different regions can be classified with three various equations of state (EoS) that are given as follows:

- Interior de-Sitter region ($0 \leq r < r_1$), with negative energy density is equal to matter pressure ($-\rho = P > 0$),
- Thin shell ($r_1 < r < r_2$) with pressure is equal to energy density ($\rho = P$), where $r_1 = C$ and $r_2 = C + \varepsilon$ are the interior and exterior radii of the gravitational vacuum star, respectively.
- Exterior vacuum Schwarzschild region ($r > r_2$) with zero pressure and energy density ($\rho = P = 0$).

Due to the presence of negative density in the interior region of the gravastar, the repulsive force is exerted on the shell wall. The shell having ultrarelativistic stiff matter introduced by Zel'dovich [7] counterbalances the force exerted by an interior zone of the collapsing star, which consequently ceases the creation of singularity inside the gravastar. The exterior vacuum region of the gravastar was studied using Reissner–Nordström or Schwarzschild metric.

Many physicists and geometers have recently become quite curious about the gravastar idea. Based on the results obtained from [4,5] motivated many researchers to analyze the structure of gravastar using different approaches. Visser et al. [6] studied the dynamical stability of the gravastar by considering three layers and concluded that there are various EoS that lead to the dynamical stability of the gravastar. Usmani et al. [8] discussed the stability of gravastar under a 2+1 dimension system and for higher dimensions in [9–11]. Rahaman et al. [12] studied the physical features of the charged gravitational vacuum star in a 2+1 system and a higher dimension with conformal motion was discussed by

^a e-mail: sanjaynenavath2016@gmail.com

^b e-mail: nmurthysk@gmail.com (corresponding author)

^c e-mail: zohrehnekouee@gmail.com

^d e-mail: manjunathahmnmt@gmail.com

Bhar [13]. Ghosh et al. [14] worked on the structure of the gravastar in the absence of conformal motion. Surface tension and negative pressure interior of a singular free black hole studied in [15]. In [16, 17], the authors explained the surface stress tensor and junction conditions on a rotating black hole. Mazur et al. [18] pose a new endpoint for gravitational collapsing stars.

As we know, Einstein's general relativity (GR) is a more suitable theory for explaining many cosmological and astrophysical phenomena. However, it is impossible to describe some observational facts such as dark energy, dark matter, and the current accelerating universe. To overcome these problems, GR needs an alternative theory as the most fruitful perspective. Among these alternative theories, $f(R)$, $f(Q)$, and $f(R, T)$ gravity made attention to many researchers analyzing the stability of the gravastar with the presence and absence of an electric field [19–24].

Electromagnetism plays an important role in studying the evaluation as well as stability of the gravitational collapsing star. Maintaining the equilibrium state for a gravastar requires an immense amount of charge to counterbalance the force exerted due to gravity acting inwards. Lobo and Arellano [25] discussed the solution and some physical features of the collapsing object along with non-linear electrodynamics. Horvat et al. [26] studied charged gravastar and evaluation adiabatic index, surface redshift, speed of sound, and EoS parameters for interior and exterior regions. Usmani et al., [10] analyzed charged gravitational vacuum star admitting conformal motion with exterior Reissnor–Nordström metric.

The conformal symmetry describes the natural relationship between matter and geometry ingredient for collapsing stars through the field equation. This inherent symmetry contained in the set of conformal Killing vectors (CKV) which is represented mathematically as

$$\mathcal{L}_\xi g_{\alpha\gamma} = \varphi(r) g_{\alpha\gamma}. \quad (1)$$

Here \mathcal{L}_ξ denotes the Lie derivative, φ is the conformal factor, and ξ represents four vectors. The CKVs play a significant role in reducing highly non-linear differential equations to linear ordinary differential equations. And also attain the exact analytic solution of the Einstein field equation more appropriately. Usmani et al. [10] discussed the exact solution of charged gravastar using conformal motion. Sharif and Arfa Waseem [27] analyzed the effect of charge on gravitational vacuum stars in $f(R, T)$ gravity and found nonsingular solutions that also describe the physical features of this star. Several authors have used a similar approach to explore more precise solutions for compact stars [28–32].

Today, Finsler geometry has become an interesting area for many researchers because of its versatility to explain various cosmological concepts, even if GR fails to explain them. Also, this geometry is the extension of Riemannian geometry. In 1935, Cartan [33] explored the model of Finsler geom-

etry and later proposed the Einstein field equation (EFE) [34] for the Cartan d -connection. Following this modified theory, numerous models [35–38] of Finsler geometry have been investigated. Nekouee et al. [35] have investigated the applications of the Finsler–Randers (FR) metric in cosmology. In recent years, numerous endeavors have taken place to study the Finsler–Randers cosmological model [40–46]. The Finslerian Schwarzschild-de sitter space-time is also recently investigated in [47]. Chowdhury et al. [48] investigated the strange stars model by considering charged fluid in the Finslerian framework. After that, Sumita Banerjee et al. [49] studied the gravastar with the background of Finslerian space-time. For all the above literature survey, here we propose the charged gravastar model with conformal motion in the framework of Finsler geometry and analyze the physical features of the gravitational collapsing star.

The structure of the current article is as follows: In Sect. 2.1, we discuss the Finsler metric structure. The structure of the Finsler gravastars is introduced in Sect. 2.2. The conformal motion of the charged gravastars is analyzed in Sect. 3. Section 4 provides a solution for the charged gravastar model in Finslerian space-time. Physical characteristics of the charged Finsler gravastar were discussed in Sect. 5. Conclusions are given in Sect. 6.

2 Structure of Finsler geometry

2.1 Finsler metric structure

The most fundamental distinction of Finsler geometry is that it incorporates the concept of anisotropic intrinsically in the geometry of space-time. The underlying space of Finsler's geometry is named Finsler space, a metric space. The metric in this space is defined as a function $F(x, y)$ from a tangent bundle of a manifold to R^1 . Here $F(x, y)$ is a non-negative function, mathematically defined as the norm instead of the inner product on a tangent bundle with the position of space-time coordinate x and a tangent vector $y \in T_x M$ representing the velocity. Hence, Finslerian geometry is dynamic geometry depending on position and direction, i.e., dynamical coordinates on a tangent bundle of a differentiable manifold, whereas Riemannian geometry is gravitational. In the framework of this type of geometry, several researchers have studied different cosmological aspects.

A Finsler space is governed by a differentiable function $F(x, y)$, also named as Finsler structure, defined on a tangent bundle TM of a manifold M as $F(x, y) : TM \rightarrow R$. The function satisfies some following properties:

- (i) F is smooth on $\tilde{TM} = TM \setminus \{0\}$, regularity property.
- (ii) F is a positive one-dimensional homogeneous function $F(x, \lambda y) = \lambda F(x, y)$ with $\lambda > 0$, homogeneity prop-

erty, where $x \in M$ and $y = \frac{dx}{d\tau}$ are the respective representation of position and velocity.

(iii) The $n \times n$ Hessian matrix

$$g_{ij} = \frac{1}{2} \dot{\partial}_i \dot{\partial}_j F^2 = \frac{1}{2} \frac{\partial}{\partial y^i} \frac{\partial}{\partial y^j} F^2. \quad (2)$$

is positive-definite at every point of $TM \setminus \{0\}$, referred as strong convexity property [50].

The geodesic spray G^ζ are expressed as,

$$G^\zeta = \frac{1}{4} g^{\zeta\mu} \left(\frac{\partial^2 F^2}{\partial x^\lambda \partial y^\mu} y^\lambda - \frac{\partial F^2}{\partial x^\mu} \right). \quad (3)$$

In the Finsler manifold, the equation of geodesic is given as,

$$\frac{d^2 x^\zeta}{d\tau^2} + 2G^\zeta = 0. \quad (4)$$

From Eq. (4), it is clear that the Finsler structure $F(x, y)$ is constant along the geodesic. The expression for Ricci tensor in the Finslerian framework is given by,

$$Ric_{\mu\nu} = \frac{1}{2} \frac{\partial^2 (F^2 Ric)}{\partial y^\mu \partial y^\nu}, \quad (5)$$

here, Ric is Ricci scalar, which is geometric invariant and is given as follows,

$$Ric = g^{\mu\nu} Ric_{\mu\nu}. \quad (6)$$

Equation (6) holds for any basis, the predecessor of the flag curvature $R_{\mu\nu}$ is represented as [51],

$$R_v^\mu = \frac{1}{F^2} \left(2 \frac{\partial G^\mu}{\partial x^v} - y^k \frac{\partial^2 G^\mu}{\partial x^k \partial y^v} + 2G^k \frac{\partial^2 G^\mu}{\partial y^k \partial y^v} - \frac{\partial G^\mu}{\partial y^k} \frac{\partial G^k}{\partial y^v} \right). \quad (7)$$

Therefore, the expression for Ric is given as,

$$Ric \equiv R_v^\nu = \frac{1}{F^2} \left(2 \frac{\partial G^\nu}{\partial x^v} - y^k \frac{\partial^2 G^\nu}{\partial x^k \partial y^v} + 2G^k \frac{\partial^2 G^\nu}{\partial y^k \partial y^v} - \frac{\partial G^\nu}{\partial y^k} \frac{\partial G^k}{\partial y^v} \right). \quad (8)$$

The expression for scalar curvature and Einstein tensor in Finslerian geometry is as follows,

$$S = g^{\mu\nu} Ric_{\mu\nu}, \quad (9)$$

$$G_{\mu\nu} = Ric_{\mu\nu} - \frac{1}{2} g_{\mu\nu} S. \quad (10)$$

Ric can be used to generate the Finslerian-modified Einstein tensor, which is insensitive to connections.

2.2 Structure of Finslerian gravastar model

To analyze the geometry of gravastar structures, we derived the Finsler structure, as given below [52],

$$F^2 = C(r)y^t y^t - D(r)y^r y^r - r^2 \tilde{F}^2(\theta, \phi, y^\theta, y^\phi), \quad (11)$$

where \tilde{F} signifies a 2-dimensional Finsler structure and \tilde{F} is specified as,

$$\tilde{F}^2 = y^\theta y^\theta + \varsigma(\theta, \phi) y^\phi y^\phi. \quad (12)$$

$$\tilde{g}_{\mu\nu} = diag \left(1, \varsigma(\theta, \phi) \right), \quad (13)$$

also, we have

$$\tilde{g}^{\mu\nu} = diag \left(1, \frac{1}{\varsigma(\theta, \phi)} \right), \quad (14)$$

where $\mu, \nu = \theta, \phi$. The Ricci scalar of Finslerian metric \tilde{F} can be derived as [43],

$$\tilde{Ric} = \frac{1}{2\varsigma} \left(-\frac{\partial^2 \varsigma}{\partial \theta^2} + \frac{1}{2\varsigma} \left(\frac{\partial \varsigma}{\partial \theta} \right)^2 \right), \quad (15)$$

which may be a function of θ or a constant (say η). We solve the Eq. (15) in three distinct conditions, and we obtained the Finsler structure \tilde{F}^2 as follows,

$$\tilde{F}^2 = y^\theta y^\theta + \mathcal{A} \sin^2(\sqrt{\eta}\theta) y^\phi y^\phi \quad (\text{for } \eta > 0), \quad (16)$$

$$\tilde{F}^2 = y^\theta y^\theta + \mathcal{A} \theta^2 y^\phi y^\phi \quad (\text{for } \eta = 0), \quad (17)$$

$$\tilde{F}^2 = y^\theta y^\theta + \mathcal{A} \sinh^2(\sqrt{-\eta}\theta) y^\phi y^\phi \quad (\text{for } \eta < 0). \quad (18)$$

Without loss of generality, we consider $\mathcal{A} = 1$. Finsler gravastar structure described in Eq. (11) can be stated as following form,

$$F^2 = C(r)y^t y^t - D(r)y^r y^r - r^2 (y^\theta y^\theta + \sin^2(\sqrt{\eta}\theta) y^\phi y^\phi). \quad (19)$$

Let α be the Riemannian metric and the associated Riemannian structure is given as,

$$\alpha^2 = C(r)y^t y^t - D(r)y^r y^r - r^2 (y^\theta y^\theta + \sin^2 \theta y^\phi y^\phi). \quad (20)$$

Equation (20) in Eq. (19) becomes,

$$F^2 = \alpha^2 + r^2 \chi(\theta) y^\phi y^\phi, \quad \text{where } \chi(\theta) = \sin^2 \theta - \sin^2(\sqrt{\eta}\theta). \quad (21)$$

Suppose we take $\beta^2 = r^2(\sin^2 \theta - \sin^2 \sqrt{\eta}\theta) y^\phi y^\phi$, in Eq. (21) we get,

$$F^2 = \alpha^2(1 + \varsigma^2), \quad (22)$$

where

$$\varsigma = \frac{\beta}{\alpha} = \frac{b_i y^i}{\alpha},$$

with $b_\phi = \sqrt{r^2(\sin^2 \theta - \sin^2 \sqrt{\eta} \theta)}$, β is a differential one-form with $b_i = (0, 0, 0, b_\phi)$. Thus Eq. (22) can be written as,

$$F = \alpha \psi(\mathfrak{s}), \quad (23)$$

here $\psi(\mathfrak{s}) = \sqrt{1 + \mathfrak{s}^2}$. Equation (23) shows that F Finsler space with a (α, β) metric.

By substituting Eq. (19) in Eq. (3) yields geodesic spray coefficients G^μ as follows,

$$G^t = \frac{C'}{2C} y^t y^r, \quad (24)$$

$$G^r = \frac{D'}{4D} y^r y^r + \frac{C'}{4D} y^t y^t - \frac{r}{2D} \tilde{F}^2, \quad (25)$$

$$G^\theta = \frac{1}{r} y^r y^\theta + \tilde{G}^\theta, \quad (26)$$

$$G^\phi = \frac{1}{r} y^r y^\phi + \tilde{G}^\phi. \quad (27)$$

where $\tilde{G}^\theta = -\frac{1}{4} \frac{\partial \zeta}{\partial \theta} y^\phi y^\phi$, $\tilde{G}^\phi = \frac{1}{4\zeta} \left(2 \frac{\partial \zeta}{\partial \theta} y^\phi y^\theta + \frac{\partial \zeta}{\partial \phi} y^\phi y^\phi \right)$.

Considering \tilde{F} as two-dimensional Finsler space-time with constant flag curvature η , using Eqs. (5), (8) and (9) in Eq. (10), one can get the components of the Einstein tensor of the modified Finsler geometry given as

$$G_t^t = \frac{D'}{rD^2} - \frac{1}{r^2D} + \frac{\eta}{r^2}, \quad (28)$$

$$G_\theta^\theta = G_\phi^\phi = -\frac{C''}{2CD} - \frac{C'}{2rCD} + \frac{D'}{2rD^2} + \frac{C'}{4CD} \left(\frac{C'}{C} + \frac{D'}{D} \right), \quad (29)$$

$$G_r^r = \frac{-C'}{rCD} - \frac{1}{r^2D} + \frac{\eta}{r^2}. \quad (30)$$

By Mazur-Mottola, the energy-momentum tensor (EMT) for isotropic pressure is as follows

$$T_v^\mu = (\rho + P)u^\mu u_\nu + Pg_v^\mu, \quad (31)$$

here, u_μ represents velocity four-vector of a fluid element (with $u_\mu u^\mu = 1$). The modified Einstein field equation for the charged fluid in Finsler geometry is given as [48],

$$G_v^\mu = \frac{8\pi_F G}{c^4} \left(T_v^\mu + E_v^\mu \right), \quad (32)$$

where T_v^μ is the EMT for matter, which is given in Eq. (31) and E_v^μ is the EMT for charge, which can be defined as

$$E_v^\mu = -\frac{1}{4\pi} \left(\mathbb{F}_{v\xi} \mathbb{F}^{\mu\xi} - \frac{1}{4} g_v^\mu \mathbb{F}_{\xi\nu} \mathbb{F}^{\xi\nu} \right). \quad (33)$$

Here $\mathbb{F}_{v\xi}$ is indicates the electromagnetic field tensor and is given by

$$\mathbb{F}_{v\xi} = \frac{\partial A_\xi}{\partial x_v} - \frac{\partial A_v}{\partial x_\xi},$$

where $\mathbb{F}_{v\xi}$ obey the Maxwell equations,

$$\mathbb{F}_{v\gamma,\xi} + \mathbb{F}_{\gamma\xi,v} + \mathbb{F}_{\xi v,\gamma} = 0,$$

and

$$\frac{\partial}{\partial x^\xi} (\sqrt{-g} \mathbb{F}^{v\xi}) = 4\pi \sqrt{-g} J^v,$$

where J^v is the current four vector, defined by $J^v = \sigma u^v$, σ is the charge density. Using Eq. (32), EFE in Finsler space-time with $G = c = 1$ is written as,

$$G_t^t = 8\pi_F T_t^t + E_t^t : \frac{D'}{rD^2} - \frac{1}{r^2D} + \frac{\eta}{r^2} = 8\pi_F \rho + E^2, \quad (34)$$

$$G_r^r = 8\pi_F T_r^r + E_r^r : \frac{-C'}{rCD} - \frac{1}{r^2D} + \frac{\eta}{r^2} = -8\pi_F P + E^2, \quad (35)$$

$$\begin{aligned} G_\mu^\mu &= 8\pi_F T_\mu^\mu + E_\mu^\mu, \quad (\mu = \theta, \phi) \frac{-C''}{2CD} \\ &\quad - \frac{C'}{2rCD} + \frac{D'}{2rD^2} + \frac{C'}{4CD} \left(\frac{C'}{C} + \frac{D'}{D} \right) \\ &= -8\pi_F P + E^2. \end{aligned} \quad (36)$$

By substituting $D = e^\lambda$ and $C = e^\nu$ in the above equations we get,

$$e^{-\lambda} \left[\frac{\lambda'}{r} - \frac{1}{r^2} \right] + \frac{\eta}{r^2} = 8\pi_F \rho + E^2, \quad (37)$$

$$e^{-\lambda} \left[\frac{1}{r^2} + \frac{\nu'}{r} \right] - \frac{\eta}{r^2} = 8\pi_F P - E^2, \quad (38)$$

$$\begin{aligned} e^{-\lambda} \left[\frac{1}{4} (\nu')^2 + \frac{\nu''}{2} - \frac{1}{4} \lambda' \nu' + \frac{1}{2r} (\nu' - \lambda') \right] \\ = 8\pi_F P + E^2, \end{aligned} \quad (39)$$

and

$$[r^2 E]' = 4\pi r^2 \sigma e^{\frac{\lambda}{2}}. \quad (40)$$

From Eq. (40), the electric field can be written as

$$E(r) = \frac{1}{r^2} \int_0^r 4\pi r^2 \sigma e^{\frac{\lambda}{2}} dr = \frac{q(r)}{r^2}, \quad (41)$$

here $q(r)$ indicates total charge of the sphere.

3 Conformal motion of the charged gravastar

Here, it is important to mention that the tensor quantity C_{ijk} plays the role of the torsion tensor in the Finslerian geometrical framework. In the study of stellar objects, for a natural

relationship between geometry and matter described by Einstein field equations, we assume an inheritance symmetry that contains a set of CKV in Finsler geometry can be expressed as [53]

$$\begin{aligned}\mathcal{L}_{\hat{\xi}}g_{\mu\nu} &= \nabla_{\mu}\xi_{\nu} + \nabla_{\nu}\xi_{\mu} + 2y^n(\nabla_n\xi^{\alpha})C_{\alpha\mu\nu} = \varphi(r)g_{\mu\nu}, \\ \nabla_{\mu}\xi_{\nu} &= \frac{\partial\xi_{\nu}}{\partial x^{\mu}} - G_{\mu}^{\alpha}\frac{\partial\xi_{\nu}}{\partial y^{\alpha}} - \Gamma_{\mu\nu}^{\alpha}\xi_{\alpha},\end{aligned}\quad (42)$$

and

$$C_{\alpha\mu\nu} = \frac{1}{4}\frac{\partial^3F^2}{\partial y^{\alpha}\partial y^{\mu}\partial y^{\nu}},$$

where \mathcal{L} indicates Lie derivative operator, $\varphi(r)$ represents the conformal vector and $\hat{\xi} = \xi^{\mu}(r)\frac{\partial}{\partial x^{\mu}} + y^{\nu}(\partial_{\nu}\xi^{\mu})\frac{\partial}{\partial y^{\mu}}$ be the vector field on TM is known as complete lift of ξ [54]. For Eq. (19), we have $C_{\alpha\mu\nu} = 0$ for all α, μ, ν . Hence, it is clear that the Cartan tensor vanishes for the metric (19).

Using Eq. (19) in (42), it gives as follows

$$\xi^r\nu' = \varphi, \quad (43)$$

$$\xi^r = \frac{r\varphi}{2}, \quad (44)$$

$$\xi^r\lambda' + 2\xi^r_{,r} = \varphi, \quad (45)$$

$$\xi^t = C_1, \quad (46)$$

implies

$$e^{\nu} = r^2C_2^2, \quad (47)$$

$$e^{\lambda} = \left(\frac{C_3}{\varphi}\right)^2, \quad (48)$$

where C_1, C_2 and C_3 are the integration constants. Plugging the above solutions in Eqs. (37–39), we get

$$\frac{1}{r^2}\left[\eta - \frac{\varphi^2}{C_3^2}\right] - \frac{2\varphi\varphi'}{rC_3^2} = 8\pi_F\rho + E^2, \quad (49)$$

$$\frac{1}{r^2}\left[\eta - \frac{3\varphi^2}{C_3^2}\right] = -8\pi_F P + E^2, \quad (50)$$

$$\frac{2\varphi\varphi'}{rC_3^2} + \frac{\varphi^2}{r^2C_3^2} = 8\pi_F P + E^2. \quad (51)$$

From Eqs. (50–51), we can get the following electric, density, and pressure terms, respectively

$$\frac{1}{2}\left(\frac{1}{r^2}\left[\eta - \frac{2\varphi^2}{C_3^2}\right] + \frac{2\varphi\varphi'}{C_3^2r}\right) = E^2, \quad (52)$$

$$\frac{\eta}{2r^2} - \frac{3\varphi\varphi'}{rC_3^2} = 8\pi_F\rho, \quad (53)$$

$$\frac{\varphi\varphi'}{rC_3^2} - \frac{1}{2r^2}\left[\eta - \frac{4\varphi^2}{C_3^2}\right] = 8\pi_F P. \quad (54)$$

4 Solution of the charged gravastar model in Finsler space-time

In this section, we have discussed the geometrical structure of the charged gravastar by three distinct regions using different EoS parameters as follows.

4.1 Interior de-sitter region of the charged gravastar

In this domain, we consider the EoS parameter $P = -\rho$, which represents the EoS for dark energy. From Eqs. (53) and (54), we get a connection between the matter variables and metric potential as below

$$\frac{2\varphi}{r^2C_3^2}(\varphi - r\varphi') = 8\pi_F(\rho + P). \quad (55)$$

Utilizing the ansatz $\rho + P = 0$ in the Eq. (55), it provides the value of φ is either $\varphi = 0$ or $\varphi = \varphi_0r$. Here, we consider the solution of conformal vector $\varphi = \varphi_0r$, which yields the exact analytical expression for all the physical variables as follows

$$-8\pi_F P = \frac{\eta}{2r^2} - 3\tilde{\varphi}_0^2 = 8\pi_F\rho, \quad (56)$$

$$E^2 = \frac{\eta}{2r^2}, \quad (57)$$

$$e^{\nu} = e^{-\lambda} = \tilde{\varphi}_0^2r^2, \quad (58)$$

$$\sigma = \frac{\sqrt{\eta}\tilde{\varphi}_0}{4\pi_F\sqrt{2}r}, \quad (59)$$

where $\tilde{\varphi}_0 = \frac{\varphi_0}{C_3}$ is a constant with the inverse dimension r .

According to Eq. (56), $\frac{\eta}{2r^2} - 3\tilde{\varphi}_0^2 > 0$ (or $\tilde{\varphi}_0 < \frac{\sqrt{\eta}}{\sqrt{6}r}$) describes the positive matter density and negative pressure, which corresponds to an outward push exerted by the interior region and is consistent with the physics of the charged gravitational collapsing star. On the other hand, $\frac{\eta}{2r^2} - 3\tilde{\varphi}_0^2 < 0$ (or $\tilde{\varphi}_0^2 < \frac{\eta}{6r^2}$) depicts a collapsing phenomenon with negative matter density and positive pressure that is not concentrated here. Thus, our above solutions satisfy criteria $0 < \tilde{\varphi}_0^2 < \frac{\eta}{6r^2}$ for the intent of a charged gravastar.

For $\tilde{\varphi}_0^2 = 0$, we evaluate the terms matter density (ρ) and pressure (P) as being inversely proportional to r but having the opposite sign along with the proportionality constant. According to Eq. (57), the electric field E is inversely proportional to r and doesn't depend on the value of $\tilde{\varphi}_0$. In another way, σ is inversely proportional to r . Both the metric potential e^{ν} and e^{λ} are proportional to r^2 as expressed in Eq. (58).

The active gravitational mass $M(r)$ for the interior domain of the charged gravastar can be given as

$$M(r) = 4\pi \int_0^r \left[\rho + \frac{E^2}{8\pi_F}\right] r^2 dr = \frac{r}{2}(\eta - \tilde{\varphi}_0^2r^2). \quad (60)$$

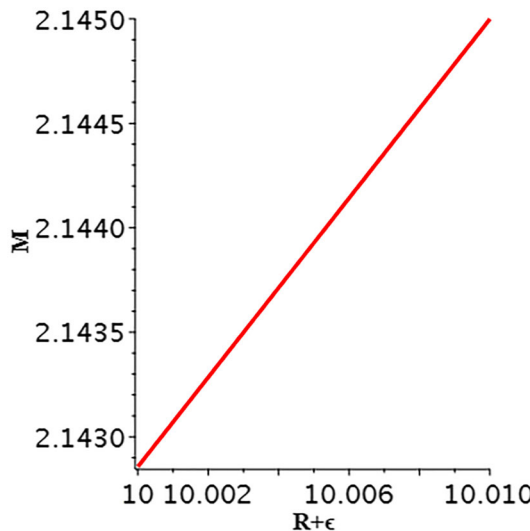


Fig. 1 Active gravitational mass M (M_\odot) with $R + \epsilon$ (km) for $\eta = 0.5$ and $\tilde{\varphi}_0^2 = \frac{\eta}{7r^2}$

This suggests that in Eq. (56), the pressure and energy density terms fail to be regular at $r = 0$ while the effective gravitational mass exhibits regular as well as positive behavior since $\tilde{\varphi}_0 < \frac{\sqrt{\eta}}{\sqrt{6}r}$ and vanishes at the origin.

It is worthwhile to observe that the physics and mathematical description of the interior region coincides with electromagnetic mass (EMM) [55]. The reason behind this is the apparent use of the electric field in the geometry of gravastar. As a result, the gravitational mass provides the force of attraction resulting from spherical collapse, which balances the repulsive force caused by the electromagnetic field.

However, in the accelerating cosmos, the equation of state parameter $P = -\rho$ represents a repulsive force that may be related to the dark energy, an agent responsible for the present phase of inflation. So, we can say that a charged gravastar provides a connection with a dark star.

4.2 Thin shell of the charged gravastar

Substituting the EoS ($P = \rho$) in Eqs. (53) and (54) we obtained the solution

$$\varphi^2 = \frac{\eta C_3^2}{2} - \frac{\varphi_1}{r}. \quad (61)$$

Here $\varphi_1 > 0$ is an integration constant. Using the preceding solution, Eqs. (52)–(54) yield

$$8\pi_F \rho = \frac{1}{2r^2} \left[\eta - \frac{3\tilde{\varphi}_1}{r} \right] = 8\pi_F P, \quad (62)$$

$$E^2 = \frac{\eta}{2r^2} - 8\pi_F \rho, \quad (63)$$

$$e^v = C_1^2 r^2, \quad (64)$$

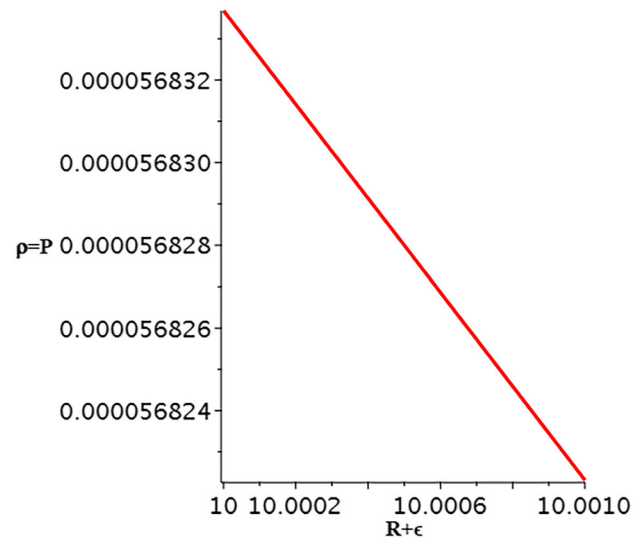


Fig. 2 Pressure-density ($\rho = P$) (km^{-2}) of the shell against $R + \epsilon$ (km) for $\eta = 0.5$ and $\tilde{\varphi}_1 = \frac{\eta r}{7}$

$$e^{-\lambda} = \frac{\eta}{2} - \frac{\tilde{\varphi}_1}{r}, \quad (65)$$

$$\sigma = \frac{\sqrt{3}\tilde{\varphi}_1}{16\pi_F r^3} \left(\sqrt{\frac{\eta r}{\tilde{\varphi}_1}} - 2 \right), \quad (66)$$

where $\tilde{\varphi}_1 = \frac{\varphi_1}{C_3^2}$ and r both have the same dimension.

In this domain, E (the electric field) is dependent on $\tilde{\varphi}_1$ and inversely proportional to r . The real value for charged density (σ) achieved only for constraint $\tilde{\varphi}_1 < \frac{\eta r}{2}$. Combining this criterion with preceding condition $\varphi_1 > 0$, we observe that the solutions for the gravastar shell region are viable only for the range $0 < \tilde{\varphi}_1 < \frac{\eta r}{2}$. It is clear from Eq. (62), which provides that the EoS ($P = \rho = 0$) for the exterior de Sitter region leads to $\tilde{\varphi}_1 < \frac{\eta r}{3}$, which is inside the range $\tilde{\varphi}_1 < \frac{\eta r}{2}$.

4.3 Exterior Schwarzschild region and matching condition

For the exterior vacuum region ($P = \rho = 0$), the Schwarzschild Finsler metric is [47]

$$F^2 = f(r) y^t y^t - \frac{1}{f(r)} y^r y^r - r^2 \tilde{F}^2(\theta, \phi, y^\theta, y^\phi), \quad (67)$$

where $f(r) = \left(1 - \frac{2MG}{\eta r}\right)$.

In the study of gravastar, a shell plays a significant role in uniting two space-time. We needed certain suitable conditions to connect the inner and exterior regions over the junction surface. These conditions are provided, by Darmois-Israel [56,57]. According to this, at the hypersurface, there has to be smooth matching between the exterior and interior domains, and the metric coefficients of both space and time are continuous at the hypersurface. But the derivative of the metric coefficient may not be. Now we evaluate the intrinsic

surface stress-energy tensor at the junction surface through the Lanczos equation [58–61] given as

$$S_v^\mu = -\frac{1}{8\pi}(H_v^\mu - \delta_v^\mu H_l^l), \quad (68)$$

where $H_{\mu\nu} = H_{\mu\nu}^+ - H_{\mu\nu}^-$ depicts the discontinuity in the extrinsic curvature or second fundamental forms. Here, the signs + and - stand for the exterior region (or Schwarzschild region) and interior region of the gravastar, respectively. The second fundamental form [62,63] is defined as follows to connect the interior and Schwarzschild outside space-time of the collapsing star on the junction surface:

$$H_{\mu\nu}^\pm = -\chi_\gamma^\pm \left[\frac{\partial^2 X_\gamma}{\partial \zeta^\mu \partial \zeta^\nu} + \Gamma_{\nu\beta}^\gamma \frac{\partial X^\nu}{\partial X^\mu} \frac{\partial X^\beta}{\partial \zeta^\nu} \right] / s, \quad (69)$$

here ζ^μ represent the intrinsic curvature coordinates, χ_γ^\pm are the unit normal on the shell surface s and are given as

$$\chi_\gamma^\pm = \pm |g^{\nu\beta} \frac{\partial f}{\partial X^\nu} \frac{\partial f}{\partial X^\beta}|^{-\frac{1}{2}} \frac{\partial f}{\partial X^\gamma}, \quad (70)$$

here $\chi^\nu \chi_\nu = 1$, ζ^μ is the intrinsic coordinate of the shell. Clearly, $f = 0$ is the parametric equation of the shell with the signs + and - indicating intrinsic and extrinsic regions of the shell, respectively.

By utilizing the Lanczos equation, we can obtain the surface stress-energy tensor as $S_{\mu\nu} = \text{diag}(\Xi, -P, -P, -P)$, where Ξ and P are the respective values for surface energy density and surface pressure and can be interpreted as following forms

$$\Xi = -\frac{1}{4\pi a} \left[\sqrt{f} \right]_-^+ \quad (71)$$

$$= -\frac{1}{4\pi a} \left[\sqrt{\eta - \frac{2MG}{a}} - \tilde{\varphi}_0 a \right], \quad (72)$$

$$P = -\frac{\Xi}{2} + \frac{1}{16\pi} \left[\frac{f'}{f} \right]_-^+ \quad (73)$$

$$= -\frac{1}{8\pi a} \left[\frac{\eta - \frac{M}{a}}{\sqrt{\eta - \frac{2M}{a}}} - \tilde{\varphi}_0 a \right], \quad (74)$$

here ($r = a$).

The surface mass of the thin shell of the charged compact object is given by

$$M_{\text{shell}} = 4\pi a^2 \Xi \quad (75)$$

$$= -a \left[\sqrt{\eta - \frac{2MG}{a}} - \tilde{\varphi}_0 a \right]. \quad (76)$$

The total mass of the gravastar is estimated by the above equation and is given below,

$$M = \frac{1}{2a} (a^2 \lambda - M_{\text{shell}}^2 + 2\tilde{\varphi}_0 a^2 M_{\text{shell}} - \tilde{\varphi}_0^2 a^4) \quad (77)$$

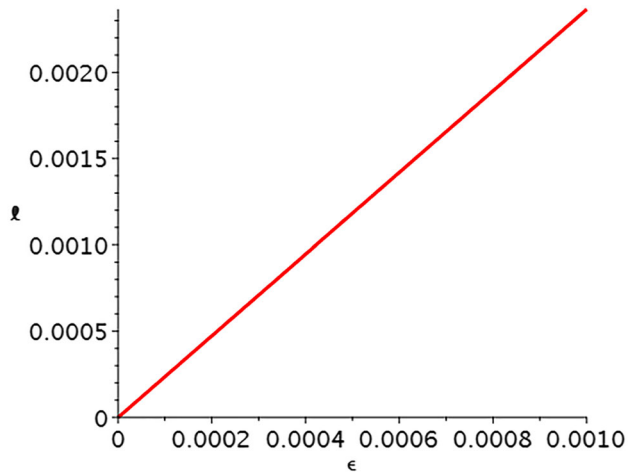


Fig. 3 Proper length ℓ (km) versus radius ϵ (km) for $\eta = 0.5$ and $\tilde{\varphi}_1 = \frac{\eta r}{7}$

5 Physical characteristics of the charged Finsler gravastars

This section examines certain necessary physical parameters that completely depict the geometry of the thin shell of the gravastar.

Proper length of the shell The proper length of the intermediate gravastar's shell connecting two regions is given as,

$$\ell = \int_R^{R+\epsilon} \sqrt{e^\lambda} dr = \left[\frac{\sqrt{2}}{\eta^{\frac{3}{2}}} \left(\varrho + \tilde{\varphi}_1 \ln \left(\frac{\varrho + \eta r - \tilde{\varphi}_1}{\sqrt{\eta}} \right) \right) \right]_R^{R+\epsilon}. \quad (78)$$

Here the inner boundary of the shell is situated at $r = R$ and the outer boundary is at $r = R + \epsilon$ ($\epsilon \ll 1$) and also $\varrho = \sqrt{(\eta r - 2\tilde{\varphi}_1)r} \sqrt{\eta}$. It is clear that for the real value of the shell thickness constant $\tilde{\varphi}_1 < \frac{\eta r}{2}$.

Energy of the shell The energy within the shell region is obtained as,

$$E^* = 4\pi_F \int_R^{R+\epsilon} \left[\rho + \frac{E^2}{8\pi_F} \right] r^2 dr = \frac{\eta}{4} [R + \epsilon - R]. \quad (79)$$

E^* proportional to the coordinate radius of the shell.

EoS parameter The EoS parameter of the shell is found by using Eqs. (72) and (74) as

$$\omega(R) = \frac{P}{\sigma} = \frac{\frac{1}{2\tilde{\varphi}_0 R} (\eta - \frac{M}{R}) - \sqrt{\eta - \frac{2M}{R}}}{\frac{1}{\tilde{\varphi}_0 R} (\eta - \frac{2M}{R}) - \sqrt{\eta - \frac{2M}{R}}} \quad (80)$$

The EoS parameter is always positive because of positive density and pressure. If for large value of R , $\omega(R) \approx 1$.

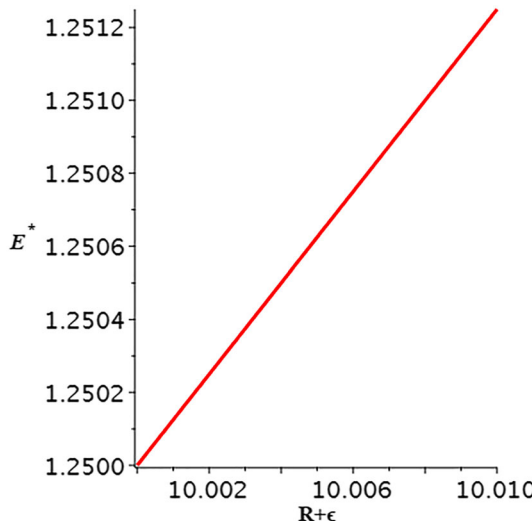


Fig. 4 The shell energy E^* (km) w.r.t thickness $R+\epsilon$ (km) for $\eta = 0.5$

Also, certain value of R in Eq. (74). We obtained $P = 0$, which represents a dust shell.

Entropy inside gravastar shell According to Mazur and Mottola [4,5], they investigated that in the interior region of the gravastar, the entropy density is zero. Using the following expression, one may determine the entropy within the gravastar shell.

$$S = 4\pi \int_R^{R+\epsilon} sr^2 \sqrt{e^\lambda} dr. \quad (81)$$

Where $s(r)$ indicates entropy density, which can be expressed as

$$\frac{\psi^2 k_B^2 T(r)}{4\pi \hbar^2 G} = \psi \left(\frac{k_B}{\hbar} \right) \sqrt{\frac{P}{2\pi G}}, \quad (82)$$

where ψ is a dimensionless constant and $T(r)$ is the radial coordinate dependent on temperature, we consider the Planck units as $\hbar = k_B = 1$. Thus the entropy of stuff matter inside the shell is

$$S = 4\pi \int_R^{R+\epsilon} r^2 \psi \left(\frac{k_B}{\hbar} \right) \sqrt{\frac{\eta}{16\pi^2 G^2} - \frac{3\tilde{\varphi}_1}{2r^3}} \sqrt{\frac{1}{\frac{\eta}{2} - \frac{\tilde{\varphi}_1}{r}}} dr \quad (83)$$

$$= \frac{\psi k_B}{\hbar G} \int_R^{R+\epsilon} r \sqrt{\frac{\eta r - 3\tilde{\varphi}_1}{\eta r - 2\tilde{\varphi}_1}} dr \quad (84)$$

If $\tilde{\varphi}_1$ tends to zero and the length of the shell is very small compared to its position from the gravastar center, then the entropy becomes $S \approx \frac{\psi k_B}{\hbar G} R \epsilon$.

Adiabatic index We might test the dynamical stability of the gravitational collapsing star with extremely small adiabatic perturbations by following the seminal work of Chandrasekhar [64]. He anticipated that the adiabatic index should

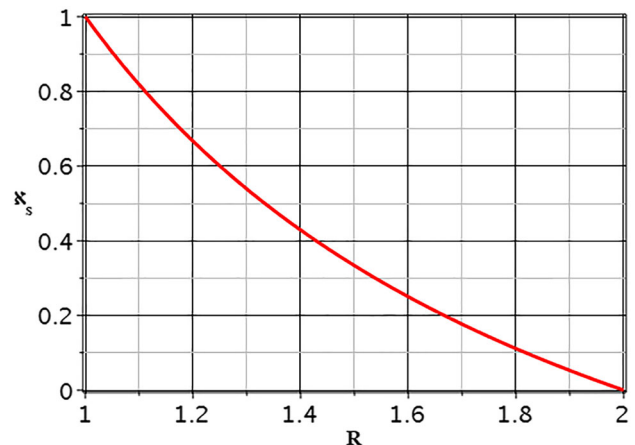


Fig. 5 Surface redshift x_s against radius R (km) for $|C_1| = 0.5$

be more than $4/3$ for the relativistic equilibrium of the system, and it is expressed as [65]

$$\Delta = \frac{P + \rho}{P} \frac{dP}{d\rho}. \quad (85)$$

Clearly, for the interior domain of the gravastar along with EoS ($P = -\rho$), the adiabatic index (Δ) should be zero, and for the thin shell region along the EoS ($P = \rho$), the adiabatic index is equal to 2.

As a result, based on the adiabatic index, we may deduce that for charged gravastars in Finslerian space-time, the inside region is unstable, and the intermediate thin shell region is stable.

Surface redshift Surface redshift for an isotropic compact star fluid cannot be greater than 2 (or cannot be greater than 5 for space-time with the present cosmological constant). It is defined as

$$x_s = |g_{tt}| - 1 = \frac{1}{|C_1| r} - 1. \quad (86)$$

6 Conclusions

In this work, we have examined charged gravitationally vacuum stars under the background of Finslerian gravity with the use of the CKV and have considered charged stellar objects with three different regions and distinct EoS parameters to analyze the structure of such objects. If the parameter $\eta = 1$, then the Finsler case is converted to the Riemannian case. We have calculated the exact analytic singular free solutions of the gravastar with CKV and derived several physical features. We have elucidated the nature of the physical parameters of the gravastar both graphically and analytically, which are listed below,

- Active gravitation mass: We have investigated the gravitational mass of the interior region of the gravastar and plotted it in Fig. 1. From this, we can see that gravitational mass increases steadily with radius, this represents that the metric function is regular and free of any singularity inside the collapsing object.
- Pressure and density profile: We have examined the pressure and density of the shell and plotted them in Fig. 2 with respect to radius. It is also worth noting that ultrarelativistic stiff fluid inside the shell is denser at the interior boundary as compared to the exterior core.
- Shell length: We calculated the shell length and sketched the graph with regard to the thickness of the shell. Figure 3 shows that the shell length of the gravastar increases with increasing shell thickness.
- Shell energy: The shell energy of the gravastar analyzed against the shell thickness, illustrated in Fig. 4, reveals that the intensity of energy increases with growing shell thickness.
- EoS parameter: The EoS parameter is positive and for a large value of R , $\omega(R) \approx 1$. Also, if we insert some particular value of R , we get $P = 0$, which represents a dust shell.
- Surface redshift: It is evident from Fig. 5 that the surface redshift is within 2. This result shows that the gravastar model is reliable and tenable from a physical standpoint.
- Adiabatic index: It is obvious from Eq. (85) that the shell is stable while the interior gravastar area is unstable.

Acknowledgements We are also grateful to the honorable referee and the editor for their valuable comments and suggestions, which have enabled us to improve the manuscript substantially.

Author contributions T. Sanjay: analysis, Plotting graphs, Writing manuscript. S. K. Narasimhamurthy and Z. Nekouee: Editing and analysis. H. M. Manjunatha: Reviewing and Editing.

Funding The author T. Sanjay acknowledges SC-ST cell, Kuvempu University, Shankaraghatta, Shivamogga, Karnataka, India, for the financial support in the form of (JRF-Ph.D) fellowship.

Data availability This manuscript has no associated data. [Author's comment: Data sharing not applicable to this article as no datasets were generated or analysed during the current study.]

Declarations

Conflict of interest The authors declare no conflict of interest.

Open Access This article is licensed under a Creative Commons Attribution 4.0 International License, which permits use, sharing, adaptation, distribution and reproduction in any medium or format, as long as you give appropriate credit to the original author(s) and the source, provide a link to the Creative Commons licence, and indicate if changes were made. The images or other third party material in this article are included in the article's Creative Commons licence, unless indicated otherwise in a credit line to the material. If material is not

included in the article's Creative Commons licence and your intended use is not permitted by statutory regulation or exceeds the permitted use, you will need to obtain permission directly from the copyright holder. To view a copy of this licence, visit <http://creativecommons.org/licenses/by/4.0/>.

Funded by SCOAP³.

References

1. J.M. Bardeen, Non singular general relativistic gravitational collapse. In *Proceedings of International Conference GR5 (Tbilise, USSR)*, p.174 (1968)
2. E. Ayón-Beato, A. García, Regular black hole in general relativity coupled to nonlinear electrodynamics. *Phys. Rev. Lett.* **80**, 5056 (1998)
3. E. Ayón-Beato, A. García, Non singular charged black hole solution for non-linear source. *Gen. Relativ. Gravit.* **629**, 31 (1999)
4. P. Mazur, E. Mottola, Gravitational condensate stars: an alternative to black hole (1988). [Arxiv:qr-qc/0109035](https://arxiv.org/abs/qr-qc/0109035). Report number: LA-UR-01-5067
5. P. Mazur, E. Mottola, Gravitational vacuum condensate stars. *Proc. Natl. Acad. Sci. USA* **101**, 9545 (2004)
6. M. Visser, D.L. Wiltshire, Stable gravastar an alternative to black holes? *Class. Quantum Gravity* **21**, 1135 (2004)
7. Y.B. Zel'dovich, A hypothesis, unifying the structure and the entropy of the universe. *Mon. Not. R. Astron. Soc.* **160**, 1 (1972)
8. A.A. Usmani et al., Variable equation of state for generalized dark energy model. *Mon. Not. R. Astron. Soc.* **386**, L92 (2008)
9. F. Rahaman et al., Singularity free dark energy star. *Gen. Relativ. Gravit.* **44**, 107 (2012)
10. A.A. Usmani et al., Charged gravastar admitting conformal motion. *Phys. Lett. B* **701**, 388 (2011)
11. F. Rahaman et al., The higher dimensional gravastar. *Int. J. Theor. Phys.* **54**, 50 (2015)
12. F. Rahaman et al., The (2+1) dimensional charged gravastars. *Phys. Lett. B* **717**, 1 (2012)
13. P. Bhar, Higher dimensional charged gravastar admitting conformal motion. *Phys. Rev. D* **78**, 104003 (2008)
14. S. Ghosh, F. Rahaman, B.K. Guha, S. Ray, Charged gravastars in higher dimensions. *Phys. Lett. B* **767**, 380 (2017)
15. P.O. Mazur, E. Mottola, Surface tension and negative pressure interior of a non-singular black hole. *Class. Quantum Gravity* **32**, 215024 (2015)
16. P. Beltracchi, P. Gondolo, E. Mottola, Surface stress tensor and junction conditions on a rotating null horizon. *Phys. Rev. D* **105**, 024001 (2022)
17. E. Mottola, Gravitational vacuum condensate stars, in *Regular Black Holes: Towards a New Paradigm of Gravitational Collapse*. ed. by C. Bambi (Springer Nature, Singapore, 2023), pp.283–352
18. P.O. Mazur, E. Mottola, Gravitational condensate stars: an alternative to black holes. *Universe* **9**, 88 (2023)
19. M.J.S. Houndjo, Reconstruction of $f(R, T)$ gravity describing matter dominated and accelerated phases. *Int. J. Mod. Phys. D* **21**, 1250003 (2012)
20. M. Sharif, Z. Yousaf, Dynamical analysis of self gravitating stars in $f(R, T)$ gravity. *Astrophys. Space Sci.* **354**, 471–479 (2014)
21. I. Noureen, M. Zubair, On dynamical instability of spherical star in $f(R, T)$ gravity. *Astrophys. Space Sci.* **356**, 103–110 (2015)
22. M. Zubair, G. Abbas, I. Noureen, Possible formation of compact stars in $f(R, T)$ gravity. *Astrophys. Space Sci.* **361**, 8 (2016)
23. A. Das et al., Gravastars in $f(R, T)$ gravity. *Phys. Rev. D* **95**, 124011 (2017)
24. M.Z. Bhatti, Z. Yousaf, T. Ashraf, Gravastars in modified Gauss–Bonnet gravity. *Chin. J. Phys.* **73**, 167–178 (2021)

25. F.S.N. Lobo, A.V.B. Arellano, Gravastars supported by non-linear electrodynamics. *Class. Quantum Gravity* **24**, 1069 (2007)

26. D. Horvat, S. Ilijic, A. Marunovic, Electrically charged gravastar configurations. *Class. Quantum Gravity* **26**, 025003 (2009)

27. M. Sharif, A. Waseem, Charged gravastars with conformal motion in $f(R, T)$ gravity. *Astrophys. Space Sci.* **364**, 189 (2019)

28. M. Esculpi, E. Aloma, Conformal anisotropic relativistic charged fluid spheres with a linear equation of state. *Eur. Phys. J. C* **67**, 521–532 (2010)

29. P. Bhar et al., Possible of higher-dimensional anisotropic compact star. *Eur. Phys. J. C* **75**, 190 (2015)

30. F. Rahaman et al., Fluid sphere: stability problem and dimensional constraint. *Int. J. Mod. Phys. D* **24**, 155049 (2015)

31. K.N. Singh et al., Effect of electric charge on anisotropic compact stars in conformally symmetric spacetime. *J. Phys. Commun.* **2**, 015002 (2018)

32. P. Bhar et al., New classes of wormhole model in $f(R, T)$ gravity by assuming conformal motion. *New Astron.* **103**, 102059 (2023)

33. E. Cartan, *Les espaces de Finsler* (Hermann, Paris, 1935)

34. J.I. Horváth, A geometrical model for the unified theory of physical fields. *Phys. Rev.* **80**, 901 (1950)

35. Z. Chang, X. Li, Modified Newton's gravity in Finsler space as a possible alternative to dark matter hypothesis. *Phys. Lett. B* **668**, 453–456 (2008)

36. S. Basilakos et al., Resembling dark energy and modified gravity with Finsler–Randers cosmology. *Phys. Rev. D* **88**, 123510 (2013)

37. F. Rahaman et al., The Finslerian wormhole models. *Eur. Phys. J. C* **76**, 246 (2016)

38. H.M. Manjunatha, S.K. Narasimhamurthy, The wormhole model with an exponential shape function in the Finslerian framework. *Chin. J. Phys.* **61**, 1561–1578 (2022)

39. Z. Nekouee et al., Finsler–Randers model for anisotropic constant-roll inflation. *Eur. Phys. J. Plus* **137**, 1388 (2022)

40. G. Papagiannopoulos et al., Finsler–Randers cosmology: dynamical analysis and growth of matter perturbations. *Class. Quantum Gravity* **34**, 225008 (2017)

41. M.K. Roopa, S.K. Narasimhamurthy, On Finsler-cosmological models in Einstein and scalar-tensor theories. *Pales. J. Math.* **9**, 957–968 (2020)

42. R. Rakesh, R. Chaubey, Finsler–Randers cosmology in the framework of a particle creation mechanism: a dynamical systems perspective. *Eur. Phys. J. Plus* **135**, 228 (2020)

43. M. Hohmann et al., Cosmological Finsler spacetimes. *Universe* **6**, 65 (2020)

44. A. Triantafyllopoulos et al., Schwarzschild-like solutions in Finsler–Randers gravity. *Eur. Phys. J. C* **80**, 1200 (2020)

45. E. Kapsabelis et al., Schwarzschild–Finsler–Randers spacetime: geodesics, dynamical analysis and deflection angle. *Eur. Phys. J. C* **82**, 1098 (2022)

46. S. Angit et al., Stability and bifurcation analysis of Finsler–Randers cosmological model. *Pramana-J. Phys.* **96**, 123 (2022)

47. H.M. Manjunatha et al., Finslerian analogue of the Schwarzschild–de Sitter space-time. *Pramana-J. Phys.* **97**, 90 (2023)

48. S.R. Chowdhury et al., Charged anisotropic strange stars in Finslerian geometry. *Eur. Phys. J. C* **79**, 547 (2019)

49. S. Banerjee et al., Study of gravastars in Finslerian geometry. *Eur. Phys. J. Plus* **135**, 185 (2020)

50. X. Li et al., Finslerian MOND versus observations of Bullet Cluster 1E 0657–558. *Mon. Not. R. Astron. Soc.* **428**, 2939–2948 (2013)

51. D. Bao, S.S. Chern, Z. Shen, *An Introduction to Riemann–Finsler Geometry* (Springer, New York, 2000)

52. X. Li, Z. Chang, Exact solution of vacuum field equation in Finsler spacetime. *Phys. Rev. D* **90**, 064049 (2014)

53. I. Bucataru, R. Miron, *Finsler–Lagrange Geometry, Applications to Dynamical Systems* (Romanian Academy Publ. House, Bucharest, 2007)

54. P. Joharinad, B. Bidabad, Conformal vector fields on Finsler spaces. *Differ. Geom. Appl.* **31**, 33–40 (2013)

55. S. Ray et al., A class of solutions for anisotropic stars admitting conformal motion. *Ind. J. Phys.* **82**, 1191 (2008)

56. G. Darmois, *Memorial des sciences mathématiques XXV, Fascicule XXV ch V* (Gauthier-Villars, Paris, 1927)

57. W. Israel, Singular hypersurfaces and thin shells in general relativity. *Nuovo Cim. B* **44**, 1 (1966)

58. K. Lanczos, Flächenhafte Verteilung der Materie in der Einstein-schen Gravitationstheorie. *Ann. Phys.* **74**, 518 (1924)

59. N. Sen, Über die Grenzbedingungen des Schwerefeldes an Unstetigkeitsflächen. *Ann. Phys.* **378**, 365 (1924)

60. G.P. Perry, R.B. Mann, Traversable wormholes in (2+1) dimensions. *Gen. Relativ. Gravit.* **24**, 305 (1992)

61. P. Musgrave, K. Lake, Junctions and thin shells in general relativity using computer algebra: I. The Darmois–Israel formalism. *Class. Quantum Gravity* **13**, 1885 (1996)

62. R. Stettner, On the stability of homogeneous, spherically symmetric, charged fluids in relativity. *Ann. Phys. (NY)* **80**, 212 (1973)

63. P.G. Whitman, R.C. Burch, Charged spheres in general relativity. *Phys. Rev. D* **24**, 2049 (1981)

64. S. Chandrasekhar, The dynamical instability of gaseous masses approaching the Schwarzschild limit in general relativity. *Astrophys. J.* **140**, 417 (1964)

65. S. Maurya, S. Maharaj, Anisotropic fluid spheres of embedding class-I using Karmarkar condition. *Eur. Phys. J. C* **77**, 328 (2017)